Optimal Properties of Bodies of Revolution in Continuum and Free Molecular Regimes

A. Dubinsky* and T. Elperin†
Ben-Gurion University of the Negev, Beer-Sheva 84105, Israel

Nomenclature

A, B	=	parameters in models for projectile–host medium interaction
a_n, a_τ	=	normal and tangent accommodation coefficients
C	=	integral force coefficient in direction $\boldsymbol{l}^0$
C_D	=	drag coefficient
C_L	=	lift coefficient
c_p	=	local pressure coefficient
c_τ	=	local tangent force coefficient
K	=	lift-to-drag ratio
$\boldsymbol{l}^0$	=	vector of direction (Fig. 1)
$\boldsymbol{n}$	=	local inner normal vector at projectile's surface
$R(x)$	=	function determining longitudinal contour of a projectile (Fig. 1)
r	=	radius of boundary cross sections of a projectile (Fig. 1)
r_1	=	base radius, reference size, m (Fig. 1)
$\boldsymbol{v}$	=	vector of freestream velocity direction (Fig. 1)
x, y, z	=	coordinates (Fig. 1)
α	=	angle of attack (see Fig. 1)
β	=	angle of inclination of longitudinal contour of a projectile (Fig. 1)
θ	=	angle in a cylindrical coordinate system (Fig. 1)
τ	=	ratio of base diameter to length of projectile
χ	=	angle determining the direction of vector $\boldsymbol{l}^0$

Subscripts

0	=	initial point of body contour
1	=	endpoint of body contour

Superscripts

0	=	unit vector
$\dot{R}$	=	derivative with respect to x
$*$	=	projectile with a minimum drag at zero incidence

Introduction

NEWTONIAN theory is successfully used in supersonic/hypersonic aerodynamics both for practical calculations and for the analysis of the effect of a projectile's shape on its local and integral aerodynamic characteristics.[1–3] The Newtonian model enables us to determine solutions that can be used in the subsequent analysis for the optimization of a projectile's shape.[4] The minimum-drag projectile with a given length and base diameter at zero incidence (ZIOP) was investigated in detail elsewhere.[5] An overview of the more recent developments is presented by Mason and Lee.[4] Because the angle of attack in real flight conditions often is not zero, it is important to investigate the behavior of the ZIOP aerodynamic characteristics at varying incidence, i.e., in nonsymmetrical flow conditions. The Newtonian model allows some useful information to be obtained. It has been shown that a local minimum or maximum of a drag for a body of revolution is attained at the angles of attack with a zero lift force.[6] It also has been found that for very blunt noses of revolution the ZIOP has the maximum (as a function of the angle of attack) lift-to-drag ratio.[7] In the present study, it is demonstrated that the ZIOP also has other optimal properties in a certain range of the angles of attack, for both the continuum and the free molecular flow regimes.

Received May 15, 1996; revision received March 7, 1997; accepted for publication March 9, 1997.

*Research Fellow, Pearlstone Center for Aeronautical Engineering Studies, Department of Mechanical Engineering, P.O. Box 653.

†Professor of Mechanical Engineering, Pearlstone Center for Aeronautical Engineering Studies, Department of Mechanical Engineering, P.O. Box 653. Member AIAA.

Basic Relations

Consider the following class of the localized interaction models[8,9] describing projectile–host medium interaction in a hypersonic flow regime:

$$c_p = At^2\delta(t), \qquad c_\tau = Bt\sqrt{1-t^2}\,\delta(t) \tag{1}$$

where $t = \boldsymbol{v}^0 \cdot \boldsymbol{n}^0$ and it is assumed that the flow interacts only with the exposed part of the projectile's surface, i.e., $\delta(t) = 1$ if $t \geq 0$, $\delta(t) = 0$ if $t < 0$. For the continuum flow regime, the parameter $B = 0$ and $A = 2$ in the classic Newtonian model. In the modified Newtonian theory for blunt bodies, A is determined by the Rayleigh formula. For a free molecular flow over a projectile with a cold surface, $A = 2(2 - a_n)$, $B = 2a_\tau$, and always $A \geq B$.

The coefficient of the integral force in a direction determined by a vector $\boldsymbol{l}^0$ (Fig. 1) is determined by integrating the local force coefficient over the lateral surface of a projectile:

$$C(\chi,\alpha) = r_0^2(A\cos\alpha\cos\chi + B\sin\alpha\sin\chi)\cos\alpha + \frac{2}{\pi}\int_0^{2/\tau}\int_0^{\pi} R(x)\cdot\delta(t_1)\left[(A-B)\frac{t_1^2 t_2}{t_0} + Bt_1\cos(\alpha-\chi)\right]\mathrm{d}x\,\mathrm{d}\theta \tag{2}$$

where

$$t_0 = \dot{R}^2 + 1, \qquad t_1 = \dot{R}\cos\alpha - \sin\alpha\cos\theta \tag{3}$$

$$t_2 = \dot{R}\cos\chi - \cos\theta\sin\chi, \qquad R(0) = r_0, \qquad R(2/\tau) = 1 \tag{4}$$

The notations are presented in Fig. 1. Hereafter, all sizes are presented in dimensionless units; the values r_1 and πr_1^2 denote a characteristic dimension and a characteristic area, respectively. We consider projectiles with a generatrix given by the increasing and convex function.

If $\alpha \leq \beta_1 = \arctan[\dot{R}(2/\tau)]$, then the lateral surface of a projectile is completely exposed and Eqs. (2–4) yield

$$C_D(\alpha) = C(\alpha,\alpha) = \tfrac{1}{2}\cos\alpha \times \left[(5\cos^2\alpha - 3)C_D(0) + (2B+3A)\sin^2\alpha\right] \tag{5}$$

$$C_L(\alpha) = C(\pi/2+\alpha,\alpha) = \tfrac{1}{2}\sin\alpha \times \left[(1 - 5\cos^2\alpha)C_D(0) + (2B+3A)\cos^2\alpha - A\right] \tag{6}$$

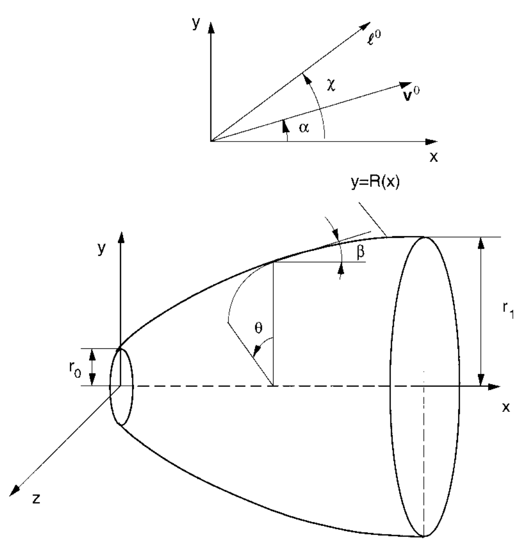

Fig. 1 Coordinates and notations.

(see, e.g., Ref. 9), where

$$C_D(0) = A - 2(A - B)\int_0^{2/\tau} \frac{R\dot{R}}{\dot{R}^2 + 1}\,\mathrm{d}x \tag{7}$$

Optimal Properties

If $A \neq B$, Eq. (7) shows that the shape of the ZIOP does not depend on parameters A and B. Therefore, the optimal projectile of Eggers et al.[5] has the minimum drag both in the continuum and in the free molecular flow regimes. In Fig. 2, we present the dependence of the angle of inclination at the base point of the generatrix vs ratio of the base diameter to the length τ for the ZIOP obtained using the solution of Eggers et al.[5]

Let us consider now a set of all bodies of revolution with a given τ with an angle of attack

$$0 < \alpha \le \alpha^* = \beta_1^*(\tau) \tag{8}$$

and assume that the lateral surface is not shadowed, i.e., Eqs. (5) and (6) are satisfied.

If $5\cos^2\alpha - 3 > 0$ ($\alpha \le \alpha_D \approx 39$ deg), then it follows from Eq. (5) that a minimum magnitude of $C_D(\alpha)$ is attained at a minimum value of $C_D(0)$. Similarly, if $1 - 5\cos^2\alpha < 0$ ($\alpha \le \alpha_L \approx 63$ deg), Eq. (6) shows that minimum $C_D(0)$ implies maximum of $C_L(\alpha)$. Thus, the minimum-drag projectile at zero incidence implies the minimum value of $C_D(\alpha)$ at all

$$\alpha \le \min\big(\alpha_D, \alpha^*\big) \tag{9}$$

the maximum value of $C_L(\alpha)$ at all

$$\alpha \le \min\big(\alpha_L, \alpha^*\big) \tag{10}$$

and, therefore, the maximum lift-to-drag ratio

$$K(\alpha) = \frac{C_L(\alpha)}{C_D(\alpha)} \tag{11}$$

at all α in the range determined by Eq. (9) for all projectiles with the same τ. Because, in reality, in the range of variation of τ, $\alpha^* < \alpha_D < \alpha_L$, conditions expressed by Eqs. (9) and (10) are reduced to the condition given by Eq. (8).

Figure 3 (see also Ref. 2) shows the dependences $C_D(\alpha)$ and $C_L(\alpha)$ given by Eqs. (5) and (6) for $B = 0$ and elucidates the essence of the parameters α_D and α_L. All of the plots $C_D(\alpha)$ and $C_L(\alpha)$ for various $C_D(0)$ intersect at points α_D and α_L, respectively. At all $\alpha < \alpha_D$, $C_D(\alpha)$ increases, and at all $\alpha < \alpha_L$, $C_L(\alpha)$ decreases when $C_D(0)$ increases.

If $A = B$ (diffuse reflection, $a_n = a_\tau = 1$), then Eqs. (2) and (7) imply the known result[2] $C_L(\alpha) = 0$ for all α and for every projectile and $C_D(\alpha) = A\cos\alpha$. Therefore, the drag coefficient of the projectile at a given α is independent of its shape if there is no shadow on its lateral surface.

The new optimal properties of the ZIOP at $\alpha \le \alpha^*$ were determined above only in the case of the projectiles without a shadow at the lateral surface. To lift the latter restriction, we use a numerical optimization. Two problems must be solved, namely, the problem of determining the minimum-drag projectile and the problem of determining the maximum-lift projectile ($A \neq B$) at a nonzero angle of attack.

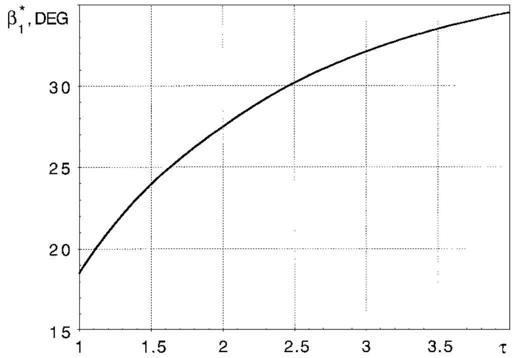

Fig. 2 Variation of the angle of inclination at the base point of the generatrix vs ratio of the base diameter to the length for the optimal projectile at zero incidence.

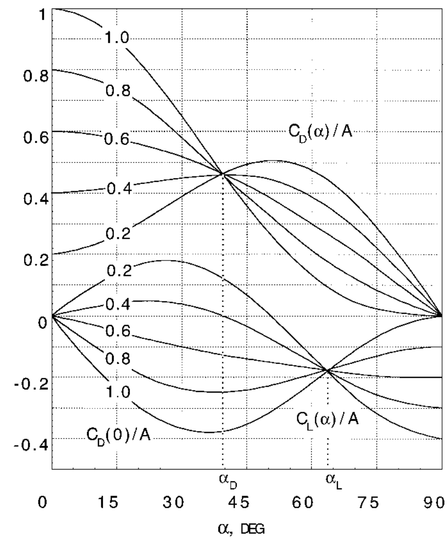

Fig. 3 Newtonian drag and lift functions.

The optimum contour is determined in the class of piecewise linear contours. To this end we constructed a uniform mesh with a constant increment $\Delta x = 2/(n\tau)$ at axis x and $\Delta y = 1/m$ at axis y. The particular contour can be specified by values $j_0, j_1, \ldots, j_n$ and the problem is reduced to determining these values such that they optimize the functional for drag (lift) coefficient. This problem was solved using a modification of the method of dynamic programming described in Ref. 9 and is applied there for determining a projectile with a minimum drag at zero angle of attack in a rarefied gas.

Calculations were performed for $n = 35$ and $m = 700$. Preliminary simulations showed that such mesh ensures that the optimal force coefficients are determined with four-digit accuracy. The magnitude of the relative thickness τ varied in the range from 1.0 to 4.0 with step 0.5, and the angle of attack α varied from in the range 0 deg to α^* with an increment ~5.0 deg. For the case when $A \neq B$, we considered the cases with $B = 0$ (Newtonian model) and with $A/B = 0.8$ (free molecular flow regime). In all cases considered, the ZIOP was obtained as the optimal projectile. For the case when $A = B$ (diffuse model), it was found that the shadow does not cause decrease of the drag coefficient.

Conclusions

Force coefficients of bodies of revolution at zero incidence were studied analytically and numerically for the hypersonic continuum flow regime (Newtonian model) and the free molecular flow regime. We showed that the minimum drag projectile at zero incidence is the same for both flow regimes and has the minimum drag, the maximum lift, and the maximum lift-to-drag ratio among the projectiles with a given length and base diameter flying at the same angle of attack. We found that in the case of a diffuse reflection in a free molecular flow regime, the drag coefficient, which is the same for all projectiles without shadow at the lateral part of the surface, does not decrease for a projectile with a shadow.

References

[1] Bertin, J. J., "State-of-the-Art Engineering Approaches to Flow Field Computations," *Hypersonics, Vol. 2: Computation and Measurement of Hypersonic Flow*, edited by J. J. Bertin, R. Glowinski, and J. Periaux, Vol. 9, Progress in Scientific Computing, 1st ed., Birhäuser, Boston, 1989, pp. 1–26.

[2] Koppenwallner, G., and Johannsmeier, D., "Behavior and Modelling of the Aerothermodynamics of Ballistic Entry Vehicles in the High Altitude Flow Regimes," *Aerothermodynamics for Space Vehicles*, Proceedings of the First European Symposium ESTEC (Noordwijk, The Netherlands), European Space Research and Technology Centre, 1991, pp. 461–467.

[3]Mason, W. H., and Lee, J., "Aerodynamically Blunt and Sharp Bodies," *Journal of Spacecraft and Rockets*, Vol. 31, No. 3, 1994, pp. 378–382.

[4]Mason, W. H., and Lee, J., "Minimum-Drag Axisymmetric Bodies in the Supersonic/Hypersonic Flow Regimes," *Journal of Spacecraft and Rockets*, Vol. 31, No. 3, 1994, pp. 406–413.

[5]Eggers, A. J., Jr., Resnikoff, M. M., and Dennis, D. H., "Bodies of Revolution Having Minimum Drag at High Supersonic Airspeeds," NACA TN 3666, 1956.

[6]Jaslow, H., "Aerodynamic Relationships Inherent in Newtonian Impact Theory," *AIAA Journal*, Vol. 6, No. 4, 1968, pp. 608–612.

[7]Pike, K., "Newtonian Aerodynamic Forces from Poisson Equation," *AIAA Journal*, Vol. 11, No. 4, 1973, pp. 499–504.

[8]Dubinsky, A., and Elperin, T., "A Simple Method for Calculating Force Coefficients of Bodies of Revolution," *Journal of Spacecraft and Rockets*, Vol. 33, No. 5, 1996, pp. 665–669.

[9]Bunimovich, A. I., and Dubinsky, A. V., *Mathematical Models and Methods of Localized Interaction Theory*, 1st ed., World Scientific, Singapore, 1995, pp. 1–45.

R. M. Cummings
Associate Editor

Extreme Value Flight Duration Analysis of Four-Engine Spacecraft

Hüseyin Sarper*
University of Southern Colorado, Pueblo, Colorado 81001

Introduction

As the United States and the other spacefaring nations are preparing a new era of exploration of nearby and distant planets, reliability issues of spacecraft will be studied more closely. New highly reliable craft that will travel long distances are needed. If such craft are crewed, the reliability concern naturally will be greater. This study considers a reliability concern given the fact that each of the engines has a life that is a random variable with known or estimated parameters. Preventive maintenance, such as performed on airplane engines, is not an option on a space voyage. The maiden flight as well as a number of subsequent flights will have to travel nonstop before space stations are built.

If each engine has a random life at some specified operating conditions such as speed and temperature, then the probability of failure and the failure rate will increase over time in the absence of preventive maintenance. Decision makers can install a fixed number (n) of such engines, some or all of which are needed to keep the spacecraft flying. As with airplane counterparts, assume that it may be possible to keep the craft flying even if one or more of the engines have failed. In this Note, n is 4 and there are two extreme types of spacecraft: one that requires all four engines to work (4 out of 4) and one that can fly with only one of the four (1 out of 4) operational. What are reliabilities or probabilities of reaching the destinations for both spacecraft when flight duration is known? For example, it may be desirable to state that the probability of being able to fly at least x time units toward the destination is $\% Y$. This probability is the reliability for a fixed flight duration.

Extreme Value Distributions

The topic of extreme value statistic[1–6] is relatively rare in most texts and articles on reliability, but this topic is important in reliability design decisions.[7] It is obvious that system failure is related to its weakest components. If such a component is essential and there are no standby units, then the system will fail as soon as the essential item fails. In a 4-out-of-4 system, for example, the system life distribution is the same as the distribution of the minimum life component. The 1-out-of-4 system, on the other hand, has a life distribution that is the same as the distribution of the maximum life component.

The analytical extreme value distribution can be derived by considering samples of size n, drawn independently and at random from a population described by its probability density function (PDF) or by its cumulative distribution function (CDF). Let the observations drawn be $\{x_1, x_2, \ldots, x_n\}$. Two statistics of interest are

$$y_n = \min\{x_1, x_2, \ldots, x_n\} \qquad \text{and} \qquad z_n = \max\{x_1, x_2, \ldots, x_n\}$$

Distribution of Smallest Values

For the 4-out-of-4 system case,

$$\begin{aligned}\text{Prob}(y_n > y) &= \text{Prob}(\text{all } x_i > y)\\ &= \text{Prob}(x_1 > y, x_2 > y, \ldots, x_n > y)\\ &= \text{Prob}(x_1 > y)\text{Prob}(x_2 > y)\cdots\text{Prob}(x_n > y)\\ &= [1 - \text{Prob}(x_1 \le y)][1 - \text{Prob}(x_2 \le y)]\\ &\quad \cdots[1 - \text{Prob}(x_n \le y)]\end{aligned}$$

Therefore, $\text{Prob}(y_n > y) = [1 - F(y)]^n$; the CDF is

$$G_n(y) = \text{Prob}(y_n \le y) = 1 - \text{Prob}(y_n > y) = 1 - [1 - F(y)]^n$$

the reliability function is

$$R_n(y) = 1 - G_n(y) = [1 - F(y)]^n$$

and the PDF is

$$g_n(y) = G_n'(y) = nf(y)[1 - F(y)]^{n-1}$$

Distribution of Largest Values

For the 1-out-of-4 system case, let the CDF be

$$\begin{aligned}H_n(z) &= \text{Prob}(z_n \le z) = \text{Prob}(\text{all } x_i \le z)\\ &= \text{Prob}(x_1 \le z, x_2 \le z, \ldots, x_n \le z) = [F(z)]^n\end{aligned}$$

The reliability function is

$$R_n(z) = 1 - H_n(z) = 1 - [F(z)]^n$$

and the PDF is

$$h_n(z) = H_n'(z) = nf(z)[F(z)]^{n-1}$$

Simulation

Simulation often helps to bypass complex mathematical work needed to reach the same result. The simulation software[8] used is a powerful tool that helps decision makers handle situations subject to uncertainty. The software[8] performs Monte Carlo simulation. Extensive use of Monte Carlo simulation in reliability work is well documented in the literature. Monte Carlo simulation is a common tool for engineers who, otherwise, face complex mathematics to deal with.

Specific Reliability Structure Under Study

The system consists of four independent engines or components. A mean life of 3000 time units and three distributions are assumed. An exponential distribution is commonly used in reliability work for illustration purposes because this distribution has a constant failure rate irrespective of duration of use. If preventive maintenance is performed, the exponential assumption is often accurate. Two other distributions, normal and uniform, are also used to consider the case when the failure rate increases over time as it would be in a long and nonstop space voyage. However, uniform and normal distributions require additional parameters. The mean life of 3000 is maintained,

Received Oct. 24, 1996; revision received Jan. 2, 1997; accepted for publication Feb. 14, 1997.

*Associate Professor of Engineering, 2200 Bonforte Boulevard. E-mail: sarper@uscolo.edu.